

Cooperative cyclic interactions involved in metal binding to pairs of sites in EF-hand proteins

Rodolfo R. Biekofsky*, James Feeney

Molecular Structure Division, National Institute for Medical Research, The Ridgeway, Mill Hill, London NW7 1AA, UK

Received 24 September 1998

Abstract This study focuses on a closed net of electron-pair donor–acceptor interactions, present in the core of all metal-bound EF-hand pairs, that link both metal ions across a short two-stranded β -sheet. A molecular model based on the above cycle of interactions was studied using semi-empirical molecular orbital quantum mechanical methods. The calculations indicate that the interactions in the model cycle are cooperative, that is, that the interaction energy of the cyclic structure is greater than that of the sum of isolated interactions between its components. The cooperativity in this cycle can be attributed to an increase in the stability of the interactions resulting from a mutual polarisation of the associated groups. The predicted polarisation of the amide groups in the cycle is in agreement with experimental NMR ^{15}N deshielding observed for these amide groups upon metal binding. Experimental observations of strengthening of the β -sheet hydrogen bonds are also consistent with the model calculations. By this mechanism, the binding of the first metal ion would enhance the binding of the second metal ion, and thus, the intradomain cooperativity in cation binding of calmodulin and related EF-hand proteins can be ascribed, at least partly, to this short-range molecular mechanism.

© 1998 Federation of European Biochemical Societies.

Key words: Calcium binding protein; EF-hand pair; Calmodulin; Cooperativity; ^{15}N nuclear magnetic resonance; Semi-empirical quantum mechanics

1. Introduction

The structures of calmodulin and other calcium binding proteins contain pairs of short sequences (helix-loop-helix motifs) normally referred to as EF-hands, placed back to back and joined as a short two-strand β -sheet unit [1]. Each EF-hand binds to a Ca^{2+} ion by coordinating the cation to a backbone carbonyl on each side of the β -sheet as well as to other ligands contained in the loop. The distance between the two bound Ca^{2+} ions is ca. 11 Å (see Fig. 1). The binding of two Ca^{2+} ions to a pair of EF-hands has been found to show positive cooperativity ([2] and references therein), where the binding of the first Ca^{2+} ion to one site enhances the affinity for Ca^{2+} of the other paired site such that the overall effect increases the response to Ca^{2+} relative to that at an isolated independent Ca^{2+} binding site. Interactions between the short antiparallel β -strands connecting the two metal binding sites could play a role in cross talk between the two sites [3]. At present, there is no detailed molecular mechanism available to explain the cooperativity in cation binding.

A cyclic net of electron-pair donor–acceptor interactions, contained in the core of a metal-bound EF-hand pair, links both metal ions across the β -sheet as shown in Fig. 1. The structural elements that form this cycle are shown in Fig. 2: these comprise the four β -sheet amide groups (two from each strand), a metal ion in each site and a side-chain carboxylate group on either side that coordinates to the corresponding metal ion in a bidentate manner. Earlier work has considered cyclic systems displaying hydrogen-bond cooperativity and attributed this to an increase of the stability of the hydrogen bonds in the cycle resulting from a mutual polarisation or charge transfer of the associated groups [4,5]. The binding energy of the cyclic structure was shown to be greater than that of the sum of individual bonds, $E(\text{A}\cdots\text{D})_n > \sum_n E(\text{A}\cdots\text{D})$, where A and D denote electron acceptor and electron donor respectively [6,7]. This leads to the question of whether or not a cycle of interactions involving two metal ions and an EF-hand pair can display similar delocalisation cooperativity since both hydrogen bonding and metal coordination are electron donor–acceptor (EDA) interactions [8].

In the present work a molecular model comprising this cycle of interactions (see Fig. 2) has been studied using semi-empirical self-consistent field (SCF) molecular orbital (MO) quantum mechanical methods. This system, although representing only a small portion of the overall structure, captures the electronic effects of a self-contained closed net of interactions. At the present state of the art, computational resources do not support the routine application of quantum mechanical methods to large molecular systems of biological interest. However, the structural trends indicated by calculations in smaller models can often shed light on molecular mechanisms relevant to the behaviour of the whole system [9–11]. The present study is aimed at reaching an improved understanding of the local interactions of the atoms involved in the ion binding process. A more detailed understanding of these interactions is of paramount importance in order to unravel the structure–function–evolution relationship of the multifunctional EF-hand family of proteins. The metal ion-induced changes in NMR ^{15}N chemical shifts for the amide NH groups in the cycle have also been analysed and correlated with the interactions in the cycle. Nuclear shielding, especially of heavier elements such as ^{15}N , is fundamentally a local phenomenon [12]. Earlier work considered experimental NMR ^{15}N shielding evidence that metal ion binding causes π -polarisation of the amide group containing the backbone carbonyl group that coordinates to the metal ion [13].

2. Materials and methods

The calculations were carried out using the PM3 parameterisation sets within the MOPAC program framework [14] sup-

*Corresponding author. Fax: (44) (181) 906-4477.
E-mail: rbiekof@nimr.mrc.ac.uk

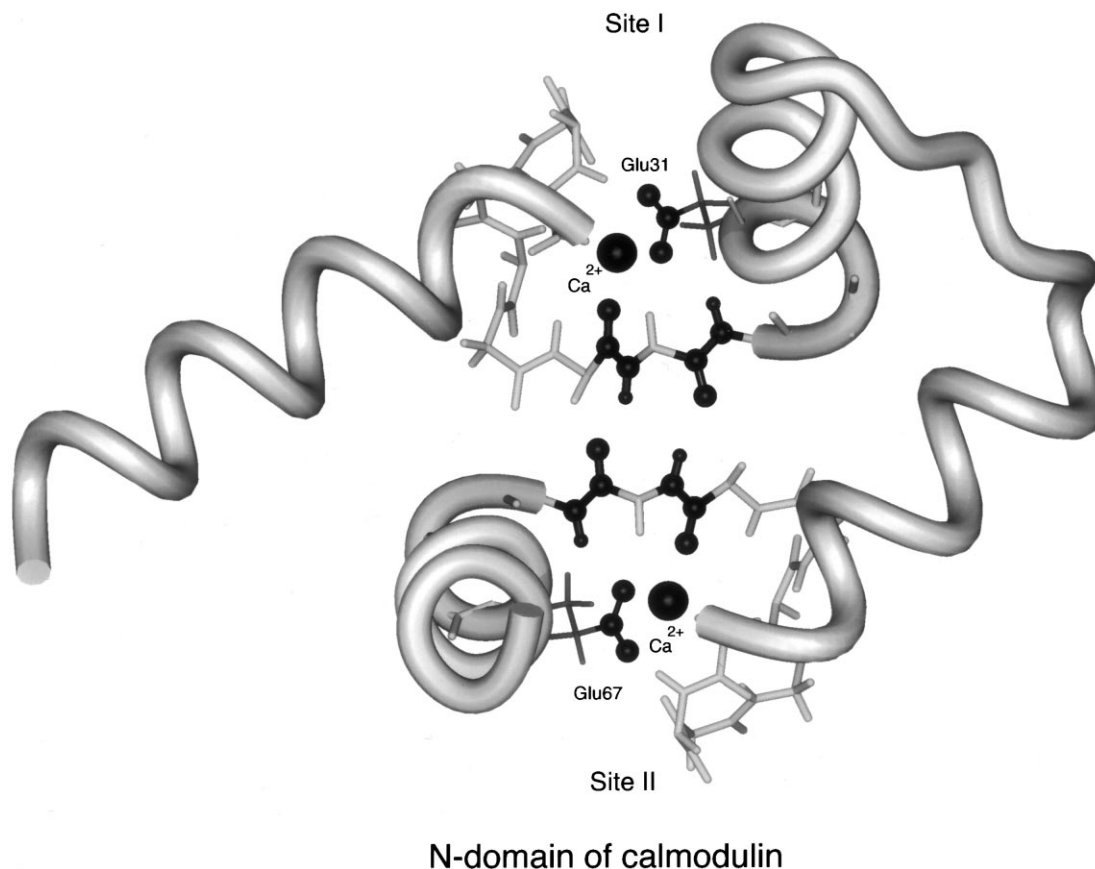


Fig. 1. Tertiary structure of N-domain of calcium-bound calmodulin from the X-ray structure reported by Rao and collaborators (1OSA in the Brookhaven PDB file) [15] showing the cycle of interactions connecting both Ca^{2+} ions across the antiparallel β -sheet in black ball-and-stick form. The backbone of the 12-residue calcium binding loop of each EF-hand is shown in stick form. The side-chain of the residue in position 12 in each EF-hand loop (Glu³¹ and Glu⁶⁷) is shown. The helices and loop between both EF-hands are shown as ribbons.

plied in the Biosym software package (Biosym Ltd.) on a Silicon Graphics INDIGO R4000 Elan/X2.

The starting coordinates for the model cycle used in the calculations were taken from the $(\text{Ca}^{2+})_4$ -calmodulin X-ray structure reported by Rao and collaborators (1OSA in the Brookhaven PDB file) [15]. Cd^{2+} , for which MOPAC semi-empirical parameters are known, was used as the metal ion (the parameters for the Ca^{2+} ion are not available) [16]. Cd^{2+} has been shown to be a good substitute for Ca^{2+} [17–22]. The side-chains for residues 7, 7', 8, 8', 9 and 9', the NH moiety for residues 7 and 7', the C=O moiety for residues 9 and 9' and the C(γ) atom for the side-chain carboxylate groups in position 12 and 12' were substituted by hydrogen atoms in the model cycle. The overall system presented a positive charge of +2.

3. Results

3.1. ^{15}N chemical shift differences

In a canonical EF-hand, a 12-residue segment contains all of the calcium binding ligands. Numbering these residues from 1 to 12, the metal binding ligands involved in the model cycle are the invariant backbone carbonyl in position 7 and the invariant glutamate bidentate carboxyl in position 12 (the other metal binding ligands in the loop are sidechain carboxamides and/or monodentate carboxylates in positions 1, 3 and

5 as well as a water molecule) [1]. In pseudo EF-hands, the binding segment is a 14-residue variation of the canonical EF-hand [23] and the ligands involved in the cycle are the invariant backbone carbonyl in position 9 and the invariant glutamate bidentate carboxyl in position 14. For simplicity, the numbering in canonical EF-hands will be used (Fig. 2).

In an earlier study, the ^{15}N chemical shifts for the amide groups CO7-NH8 and CO7'-NH8' in a number of EF-hand proteins were examined and the changes in ^{15}N shielding upon metal binding were tabulated ([13], and references therein). The deshielding of these ^{15}N nuclei upon metal binding (+4 to +8 ppm) is consistent with a π -polarisation of these amide groups upon coordination of the metal ions to the carbonyls in positions 7 and 7' ([13], and references therein). The ^{15}N chemical shifts for amide groups CO8-NH9 and CO8'-NH9' of a number of EF-hand proteins have now been examined and the changes in ^{15}N shielding accompanying metal binding are shown in Table 1. These ^{15}N nuclei show a deshielding effect of +2 to +8 ppm. Because both the NH as well as the C=O of these amide groups are involved in hydrogen bonding, the π -polarised resonance form of this amide group would be expected to be stabilised and the polarisation can be related to the observed deshielding effect [5,12]. The ^{15}N deshielding effects for the four amide groups involved in the cycle are observed to be very similar for the binding of either Ca^{2+} or Cd^{2+} [20,24].

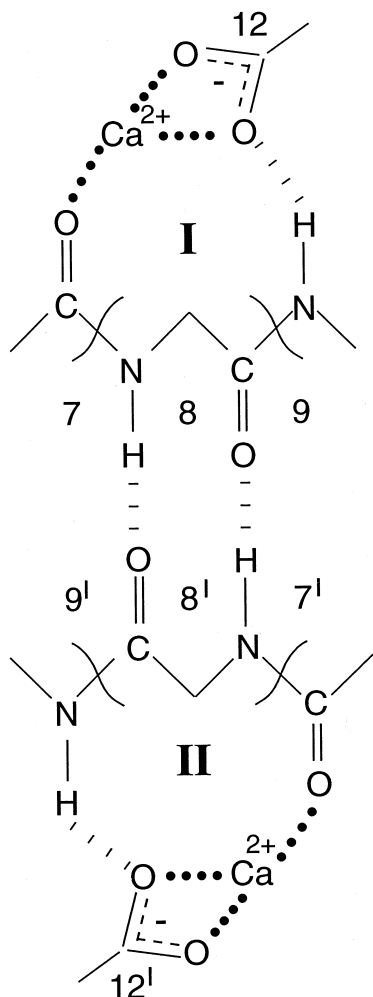


Fig. 2. Schematic drawing of antiparallel β -sheet characteristic of EF-hand pairs showing cycle of interactions upon Ca^{2+} binding to both sites in a canonical EF-hand pair. Numbers indicate the position of the residues in each calcium binding loop. Primed numbers correspond to calcium binding site II.

3.2. Quantum mechanical calculations

The geometry for the model cycle was optimised using MO-PAC-PM3 and is shown in Fig. 3. The calculations on the model system indicate π -polarisation of the amide groups in the cycle. This can be seen from the shortening of the C–N bond and lengthening of the N–H and C–O bonds (Table 2), as well as from the charges on the amide N and H atoms (becoming more positive) and on the amide O atoms (becoming more negative) (Table 3). This result is in agreement with the experimental observation of ^{15}N deshielding for the four amide groups involved in the cycle and is consistent with simultaneous stabilisation of the polarised resonance forms for the four amide groups in the cycle (Fig. 4). The polarisations of the electron donor–acceptor pairs involved in the cycle run in the same direction (homodromic orientation) [5], as shown in Fig. 4.

The calculations predict shortening, and hence strengthening, of the β -sheet hydrogen bonds in the model cycle as compared with the same interactions in the β -strand without the $\text{Cd}^{2+}/\text{COO}^-$ pairs (a model for the apo form) (Table 2). Due to the simultaneous polarisation of the amide groups in the cycle, the amide oxygen atoms become more negative enhancing their electron-donor ability and the amide NH atoms become more positive enhancing their electron-acceptor ability. Thus, the donor–acceptor interactions in the cycle, in particular, the β -sheet hydrogen bonds, become enhanced [5]. This is in agreement with experimental observations in EF-hand proteins which have indicated that the β -sheet hydrogen bonds are stronger in the calcium-bound form than in the apo form. Proton exchange rates of the β -sheet amide NH groups in calbindin D_{9k} are observed to decrease upon Ca^{2+} binding indicating strengthening of these hydrogen bonds [25]. NOEs between the β -strands found in calcium-bound calmodulin are either absent or weakened in the apo state of calmodulin consistent with a more flexible and mobile apo state [26–28]. The short β -sheet between calcium binding sites III and IV in cardiac troponin C was found to be disrupted or weakened in the absence of Ca^{2+} , based on proton chemical shift analysis [29].

In order to evaluate the cooperativity of the interactions in the model cycle, the energy quantities $E(\text{A}\cdots\text{D})_n$ and Σ_n

Table 1

^{15}N chemical shifts for the NH residue in position 9 of canonical EF-hand loops or 11 in pseudo EF-hand loops

Protein	Site I (or III)					Site II (or IV)				
	pos ^a	res ^a	$\delta(\text{Ca}^{2+})_2^b$	$\delta(\text{apo})^b$	$\Delta\delta(\text{h}-\text{a})^c$	pos ^a	res ^a	$\delta(\text{Ca}^{2+})_2^b$	$\delta(\text{apo})^b$	$\Delta\delta(\text{h}-\text{a})^c$
(A) Ca^{2+} -loaded and Ca^{2+} -free forms										
Calmodulin ^{d,e}	9	T28	116.6	111.2	+5.4	9	D64	128.3	124.6	+3.7
Calmodulin ^{d,e}	9	S101	123.8	118.0	+5.8	9	N137	129.0	125.7	+3.3
N-troponin C ^f	9	S38	124.0	115.8	+8.2	9	D74	131.9	126.0	+5.9
Calbindin ^{g,h}	11	S24	120.9	119.3	+1.6	9	S62	126.5	120.4	+6.1
(B) Cd^{2+} -loaded and apo forms in calbindin D_{9k}										
	pos ^a	res ^a	$\delta(\text{Cd}^{2+})_2^b$	$\delta(\text{apo})^b$	$\Delta\delta(\text{h}-\text{a})^c$	pos ^a	res ^a	$\delta(\text{Cd}^{2+})_2^b$	$\delta(\text{apo})^b$	$\Delta\delta(\text{h}-\text{a})^c$
Calbindin ^h	11	S24	n.d. ^a	119.3	*	9	S62	125.4	120.4	+5.0

^aAbbreviations: pos, position in the EF-hand loop; res, residue type and number in the protein; n.d., not determined.

^b $\delta(\text{Ca}^{2+})_2$, $\delta(\text{Cd}^{2+})_2$, $\delta(\text{apo})$: ^{15}N chemical shift (in ppm referenced to liquid NH_3) for the NH in Ca^{2+} -loaded, Cd^{2+} -loaded and metal-free form respectively.

^c $\Delta\delta(\text{h}-\text{a})$: ^{15}N chemical shift difference (in ppm) of Ca^{2+} -loaded (holo) minus Ca^{2+} -free (apo) forms (A) and Cd^{2+} -loaded (holo) minus apo forms (B).

^dData for holo-calmodulin taken from [43].

^eData for apo-calmodulin (M. Ikura, personal communication).

^fData for holo- and apo N-troponin C taken from [44].

^gData for $(\text{Ca}^{2+})_2$ and apo-calbindin D_{9k} taken from [24].

^hData for $(\text{Cd}^{2+})_2$ calbindin D_{9k} taken from [20].

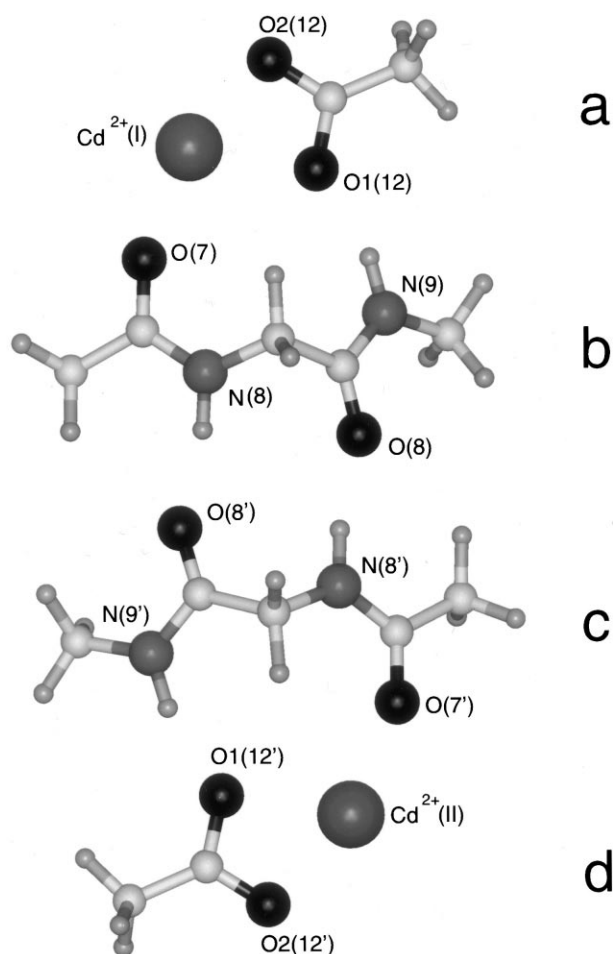


Fig. 3. Optimised geometry of model cycle of interactions using MOPAC-PM3. Components are indicated by **a**, **b**, **c** and **d**.

$E(A\cdots D)$ were estimated from the MOPAC-PM3 calculations. The total interaction energy $E(A\cdots D)_n$ is calculated as the energy of the optimised cyclic system minus the energy of the isolated components. A component in this case is a portion of the total system not bound by covalent bonds to the rest of the structure and presenting the same geometry as in the optimised cycle. The cycle can be thought of as being constituted of four components **a**, **b**, **c** and **d** as shown in Fig. 3: **a**, $\text{Cd}^{2+}/\text{COO}^-$ for site I, **b**, β -strand for site I, **c**, β -strand for site II and **d**, and $\text{Cd}^{2+}/\text{COO}^-$ for site II. The calculations on the model cycle system gave a value of -19.30 kcal/mol for the total interaction energy of the cyclic system $E(A\cdots D)_n$.

The energies of the individual interactions were calculated

for all pairs of components in order to estimate $\sum_n E(A\cdots D)$, the sum of the energies of the isolated interactions. The interaction energy between for example components **a** and **b** was calculated as the energy for **a** and **b** together minus the energy for the isolated component **a** and minus the energy for the isolated component **b**. In this way, the interaction energy for the isolated interaction between **a** and **b** is found to be -16.17 kcal/mol. This encompasses the interactions of $\text{C}=\text{O}(7)$ coordination to Cd^{2+} and the H-bonding of $\text{NH}(9)$ to $\text{COO}^-(12)$. Similarly, the interaction energy for the isolated interaction between **c** and **d** is -16.17 kcal/mol. For **b** and **c**, the interaction energy for the isolated interaction between both β -sheet strands is -6.50 kcal/mol. For the isolated interaction between both $\text{Cd}^{2+}/\text{COO}^-$ pairs, that is **a** and **d**, the isolated interaction energy is $+26.03$ kcal/mol. This last energy term is positive since it is an electrostatic repulsive interaction between two positively charged components. The sum of the isolated interaction energies on the model cycle system, $\sum_n E(A\cdots D)$, is estimated to be -12.81 kcal/mol by the MOPAC-PM3 calculations.

Hence, the calculations on the model cycle indicate that the total interaction energy of the cyclic system, $E(A\cdots D)_n = -19.30$ kcal/mol, is greater than the sum of the isolated interactions, $\sum_n E(A\cdots D) = -12.81$ kcal/mol. The difference between $E(A\cdots D)_n$ and $\sum_n E(A\cdots D)$ gives an estimate of the cooperative stabilisation in this cycle of -6.49 kcal/mol. This kind of analysis has been previously reported for cooperative hydrogen-bonded cycles [6,7].

4. Discussion

The present study introduces a novel type of cooperative cycle of interactions involving metal ions, which suggests a possible molecular mechanism contributing to the cooperativity in cation binding of EF-hands. The calculations indicate that the interactions in the model cycle are cooperative, that is, that the interaction energy of the cyclic structure is greater than that of the sum of isolated interactions between its components. The cooperativity in this cycle can be attributed to an increase in the stability of the interactions resulting from a mutual polarisation of the associated groups. By this mechanism, the binding of the first Ca^{2+} ion would enhance the binding of the second Ca^{2+} ion. The calculated polarisation in the four β -sheet amide groups in the cycle is consistent with the observed ^{15}N deshielding accompanying Ca^{2+} binding, suggesting that this molecular mechanism is present in EF-hand proteins binding to metals. Additionally, experimental observations indicative of strengthening of the β -sheet hydrogen bonds upon metal binding in EF-hand proteins (see above) are also consistent with the results of the calculations

Table 2
Calculated bond lengths (\AA) for β -sheet amide groups in the model cycle (Fig. 2) and in the apo model

Bond	Cycle	Apo	$\Delta(c-a)^a$	Bond	Cycle	Apo	$\Delta(c-a)^a$
O(7)=C(7)	1.265148	1.228374	+0.036774	O(7')=C(7')	1.265037	1.228350	+0.036687
C(7)-N(8)	1.369336	1.407981	-0.038645	C(7')-N(8')	1.369411	1.408085	-0.038674
N(8)-H(8)	1.018261	1.015898	+0.002363	N(8')-H(8')	1.018324	1.015942	+0.002382
H(8) \cdots O(8')	1.789935	1.805579	-0.015644	H(8') \cdots O(8)	1.789938	1.805332	-0.015394
O(8')=C(8')	1.238850	1.234336	+0.004514	O(8)=C(8)	1.238777	1.234292	+0.004485
C(8')-N(9')	1.379873	1.392808	-0.012935	C(8)-N(9)	1.379874	1.392765	-0.012891
N(9')-H(9')	1.014372	0.997191	+0.017181	N(9)-H(9)	1.014427	0.997223	+0.017204

^a $\Delta(c-a)$: difference in bond length between cycle and apo model.

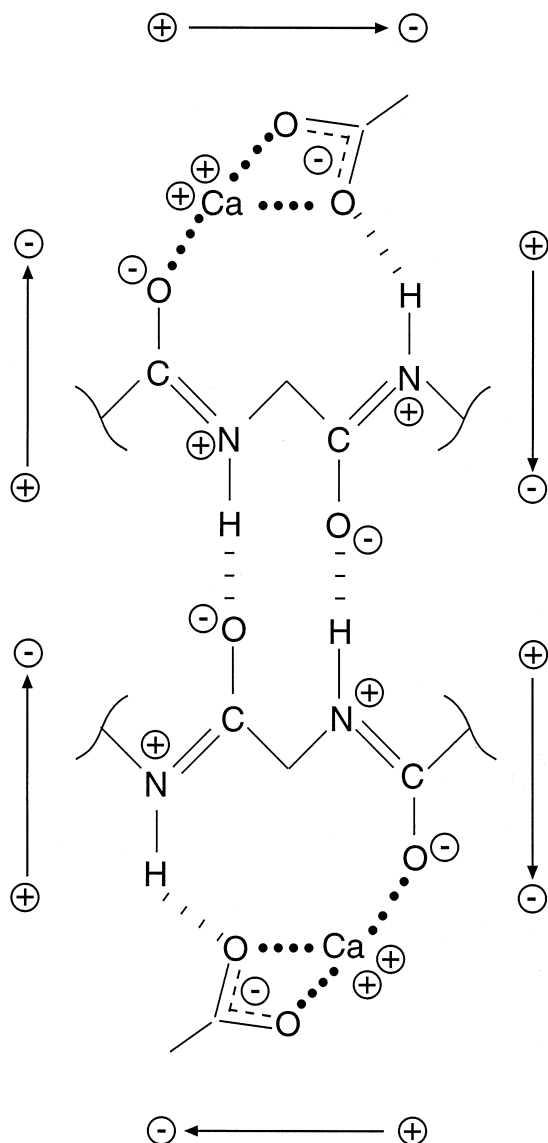


Fig. 4. Main canonical structure of resonance of amide groups involved in cycle of interactions. Binding of cation–carboxylate pairs to both sides of the β -sheet stabilise the polarised resonance structure of the amide groups. The arrows from + to – indicate the array of dipoles in the cycle.

in the model cycle, suggesting that the cyclic molecular mechanism occurs in metal-bound EF-hand pairs.

For calmodulin, the simultaneous polarisation of the β -sheet amide groups in the cycle within each domain can be followed throughout the calcium titration of the apo protein. The calcium binding curves obtained from measurements of

position 8 NH signals for the pair of sites within each domain were found to change in parallel [13]. This is consistent with positive intradomain cooperativity of calcium binding indicating that the predominant species present during the titration are $[\text{Ca}_0^{\text{N}}\cdot\text{Ca}_0^{\text{C}}]\text{CaM}$, $[\text{Ca}_0^{\text{N}}\cdot\text{Ca}_2^{\text{C}}]\text{CaM}$ and $[\text{Ca}_2^{\text{N}}\cdot\text{Ca}_2^{\text{C}}]\text{CaM}$ (Ca_x^{N} and Ca_x^{C} indicate the number of bound calcium ions bound to either the N- or C-domain respectively). This behaviour indicates that within each domain the cycle of interactions containing two calcium ions is also formed at partial degrees of calcium saturation.

The formation of a circular net of interactions would also provide a driving force for the dimerisation of isolated calcium binding loops observed upon the addition of lanthanides [30]. The 12-residue synthetic analogue of calcium binding loop III of calmodulin synthesised by Wójcik and coworkers was found to undergo a metal ion-induced folding transition. The absence of metal ions favours a random coil conformation for this peptide, whereas the La^{3+} ions are able to lock down the liganding groups tightly and maintain a rigid structure that can dimerise and bind La^{3+} ions cooperatively [30]. The dimer structure was found to be similar to that of two-loop structural elements in native EF-hand proteins: at the interface of the loops the residues at position 8 form a short antiparallel β -sheet. The ‘extra’ stabilisation gained by closing the cycle of interactions with both bound metal ions provides an explanation for the formation of these dimers in the absence of interhelical contacts.

The calculations indicate that the cooperativity in cation binding of EF-hand pairs can be ascribed at least partly to the short-range cooperative interactions of the model cycle. Another mechanism that has been proposed to contribute to the cooperativity in cation binding involves inter-motif helix pairings: in this mechanism concerted conformational changes through the helix pairs between adjacent EF-hand motifs could allow one EF-hand to transfer Ca^{2+} binding information to the other EF-hand [28,31]. The cooperative cycle of interactions connecting both metal ions discussed above would seem to complement and reinforce the inter-motif helix mechanism. The cooperativity of the interactions in the cycle enhances the binding of the metal ion and of the bidentate carboxylate group in each site. The invariant glutamate in position 12, coordinated to the Ca^{2+} ion in a bidentate manner, forms part of the first turn of the second helix of the EF-hand motif (the ‘F helix’) (see Fig. 1). In the calcium-free structure of calmodulin, the carboxylate oxygens of this glutamate appear to be several angstroms farther away from their positions in the Ca^{2+} -ligated structure [28]. The coordination of the bidentate carboxylate oxygen atoms to the metal ion requires a change in the backbone conformation in this region, which could trigger the reported conformational rearrangement in the calmodulin domains from the ‘closed’ apo

Table 3

Calculated electronic charges on oxygen, nitrogen and NH hydrogen atoms of β -sheet peptide groups in the model cycle (Fig. 2) and in apo model

Atom	Cycle	Apo	$\Delta(\text{c}-\text{a})$	Atom	Cycle	Apo	$\Delta(\text{c}-\text{a})$
O(7)	–0.6496	–0.3797	–0.2699	O(7')	–0.6496	–0.3797	–0.2699
N(8)	+0.0386	–0.0376	+0.0762	N(8')	+0.0383	–0.0376	+0.0759
H(8)	+0.1771	+0.0886	+0.0885	H(8')	+0.1771	+0.0886	+0.0885
O(8')	–0.4786	–0.3885	–0.0901	O(8)	–0.4784	–0.3885	–0.0899
N(9')	–0.0009	–0.0255	+0.0246	N(9)	–0.0009	–0.0255	+0.0246
H(9')	+0.1480	+0.0788	+0.0692	H(9)	+0.1481	+0.0788	+0.0693

^a $\Delta(\text{c}-\text{a})$: difference in bond length between cycle and apo model.

state to the 'open' Ca^{2+} -ligated state [28]. The binding of the glutamate-12 carboxylate groups to the Ca^{2+} ions appears to be involved with the motion of the 'F helices' in both EF-hands, so that the ends of these helices nearer to the β -sheet come close together and the opposite ends of these helices move away from one another [32]. The interdependence and relative contribution of these synergetic mechanisms to the overall phenomenon of cooperativity in cation binding is of great interest in the field of calcium binding proteins and forms a basis for further investigation.

Since the Mg^{2+} ion does not trigger calcium proteins [33,34], it is tempting to think that the cooperative cycle operates as a selective mechanism that promotes tight Ca^{2+} binding allowing Ca^{2+} to compete successfully even in the presence of a high Mg^{2+} concentration. The cycle of interactions involves a backbone $\text{C}=\text{O}$ and a bidentate COO^- as calcium ligands in both binding sites. The smaller Mg^{2+} ion preferentially binds highly negatively charged ligands with strictly sixfold octahedral coordination geometry and cannot easily accommodate a neutral carbonyl and an irregular bidentate carboxylate within its sphere of coordination [35,36]. The cycle of interactions appears not to be formed with Mg^{2+} : from the ^1H - ^{15}N HSQC spectra shown by Ohki and collaborators it can be observed that the residues in position 9 of the calcium binding loops in calmodulin (residues T28, D64, S101 and N137) do not show a shift for their amide ^{15}N signal upon excess addition of Mg^{2+} to the apo protein [33]. Hence, the corresponding CO8-NH9 amide groups appear not to polarise upon addition of Mg^{2+} , contrary to that observed for the addition of Ca^{2+} . A polarisation of this amide group would be expected if the carboxylate in position 12 is hydrogen-bonded to the NH in position 9 (see Fig. 2). The critical role of the bidentate carboxylate has been highlighted by the several studies involved with the mutation of the position 12 glutamate in individual Ca^{2+} binding sites of calmodulin [37,38], troponin C [39,40] and calbindin D_{9k} [41]. The invariance and unique interaction network of the backbone $\text{C}=\text{O}$ and the bidentate COO^- in each calcium binding loop [42] suggests that the cooperative cycle appeared early in the evolution of calcium binding proteins and remained as an essential feature for their function.

Acknowledgements: We are grateful to Peter M. Bayley (NIMR, Mill Hill), Franca Fraternali (NIMR, Mill Hill), Jens Kleinjung (NIMR, Mill Hill), Poul Erik Hansen (Roskilde University, Denmark) and Annalisa Pastore (NIMR, Mill Hill) for critical reading of the manuscript. This work was supported by funds from the Medical Research Council. R.R.B. was supported by a Marie Curie Fellowship from the Commission of the European Communities and a Travelling Research Fellowship from the Wellcome Trust.

References

- [1] Strydom, N.C.J. and James, M.N.G. (1989) *Annu. Rev. Biochem.* 58, 951–998.
- [2] Linse, S. and Chazin, W.J. (1995) *Protein Sci.* 4, 1038–1044.
- [3] Wesolowski, T.A., Boguta, G. and Bierynski, A. (1990) *Protein Eng.* 4, 121–124.
- [4] Saenger, W. (1979) *Nature* 279, 343–344.
- [5] Jeffrey, G.A. and Saenger, W. (1991) *Hydrogen bonding in Biological Structures*, Springer Verlag, Berlin.
- [6] Lesyng, B. and Saenger, W. (1981) *Biochim. Biophys. Acta* 678, 408–413.
- [7] Koehler, J.E.H., Saenger, W. and Lesyng, B. (1987) *J. Comp. Chem.* 8, 1090–1098.
- [8] Glusker, J.P. (1991) *Adv. Protein Chem.* 42, 1–76.
- [9] Polshakov, V.I., Birdsall, B., Gradwell, M.J. and Feeney, J. (1995) *J. Mol. Struct. (Theochem.)* 357, 207–216.
- [10] Nishihira, J. and Tachikawa, H. (1997) *J. Theor. Biol.* 185, 157–163.
- [11] Harrison, M.J., Burton, N.A. and Hillier, I.H. (1997) *J. Am. Chem. Soc.* 119, 12285–12291.
- [12] De Dios, A.C., Pearson, J.G. and Oldfield, E. (1993) *Science* 260, 1491–1496.
- [13] Biekofsky, R.R., Martin, S.R., Browne, J.P., Bayley, P.M. and Feeney, J. (1998) *Biochemistry* 37, 7617–7629.
- [14] Stewart, J.J.P. (1989) *J. Comp. Chem.* 10, 209–220.
- [15] Rao, S.T., Wu, S., Satyshur, K.A., Ling, K.-Y., Kung, C. and Sundaralingam, M. (1993) *Protein Sci.* 2, 436.
- [16] MOPAC7 (1997) Quantum Chemistry Program Exchange (QCPE) (Counts R., Ed.), Department of Chemistry, Indiana University, Bloomington, IN.
- [17] Teleman, O., Drakenberg, T., Forsén, S. and Thulin, E. (1983) *Eur. J. Biochem.* 134, 453–457.
- [18] Swain, A.L., Kretsinger, R.H. and Amma, E.L. (1989) *J. Biol. Chem.* 264, 16620–16628.
- [19] Zhang, C.Y. and Nelson, D.J. (1992) *J. Alloys Compounds* 180, 349–356.
- [20] Akke, M., Forsén, S. and Chazin, W.J. (1993) *Magn. Reson. Chem.* 31, S128–S132.
- [21] Linse, S., Bylsma, N.R., Drakenberg, T., Sellers, P., Forsén, S., Thulin, E., Svensson, L.A., Zajtzeva, I., Zajtsev, V. and Marek, J. (1994) *Biochemistry* 33, 12478–12486.
- [22] Akke, M., Forsén, S. and Chazin, W.J. (1995) *J. Mol. Biol.* 252, 102–121.
- [23] Schäfer, B.W. and Heizmann, C.W. (1996) *Trends Biochem. Sci.* 21, 134–140.
- [24] Skelton, N.J., Akke, M., Kördel, J., Thulin, E., Forsén, S. and Chazin, W.J. (1992) *FEBS Lett.* 303, 136–140.
- [25] Linse, S., Teleman, O. and Drakenberg, T. (1990) *Biochemistry* 29, 5925–5934.
- [26] Ikura, M., Minowa, O. and Hikichi, K. (1985) *Biochemistry* 24, 4264–4269.
- [27] Urbauer, J.L., Short, J.H., Dow, L.K. and Wand, A.J. (1995) *Biochemistry* 34, 8099–8109.
- [28] Zhang, M., Tanaka, T. and Ikura, M. (1995) *Nature Struct. Biol.* 2, 758–767.
- [29] Krudy, G.A., Brito, R.M.M., Putkey, J.A. and Rosevear, P.R. (1992) *Biochemistry* 31, 1595–1602.
- [30] Wójcik, J., Góral, J., Pawlowski, K. and Bierynski, A. (1997) *Biochemistry* 36, 680–687.
- [31] Travé, G., Lacombe, P.-J., Pfuhl, M., Saraste, M. and Pastore, A. (1995) *EMBO J.* 14, 4922–4931.
- [32] Finn, B.E., Evenäs, J., Drakenberg, T., Waltho, J.P., Thulin, E. and Forsén, S. (1995) *Nature Struct. Biol.* 2, 777–783.
- [33] Ohki, S., Ikura, M. and Zhang, M. (1997) *Biochemistry* 36, 4309–4316.
- [34] Andersson, M., Malmendal, A., Linse, S., Ivarsson, I., Forsén, S. and Svensson, L.A. (1997) *Protein Sci.* 6, 1139–1147.
- [35] Martin, R.B. (1984) in: *Calcium and Its Role in Biology* (Siegel, H., Ed.), pp. 1–49, Marcel Dekker, New York.
- [36] Da Silva, J.J.R.F. and Williams, R.J.P. (1991) *The Biological Chemistry of the Elements*, Clarendon Press, Oxford.
- [37] Maune, J.F., Klee, C.B. and Beckingham, K. (1992) *J. Biol. Chem.* 267, 5286–5295.
- [38] Evenäs, J., Thulin, E., Malmendal, A., Forsén, S. and Carlström, G. (1997) *Biochemistry* 36, 3448–3457.
- [39] Gagné, S.M., Li, M.X. and Sykes, B.D. (1997) *Biochemistry* 36, 4386–4392.
- [40] Li, M.X., Gagné, S.M., Spyropoulos, L., Kloks, C.P.A.M., Audette, G., Chandra, M., Solaro, R.J., Smillie, L.B. and Sykes, B.D. (1997) *Biochemistry* 36, 12519–12525.
- [41] Carlström, G. and Chazin, W.J. (1993) *J. Mol. Biol.* 231, 415–430.
- [42] Moncrief, N.D., Kretsinger, R.H. and Goodman, M. (1990) *J. Mol. Evol.* 30, 522–562.
- [43] Ikura, M., Kay, L.E. and Bax, A. (1990) *Biochemistry* 29, 4659–4667.
- [44] Li, M.S., Gagné, S.M., Tsuda, S., Kay, C.M., Smillie, L.B. and Sykes, B.D. (1995) *Biochemistry* 34, 8330–8340.